Structural, Electrical and Optical Characteristics of $Zn_{100-x}Cd_xO$ Thin Films

Hend Alkhammash[1*], H. Abd El-Ghanny[2], M. M. Abd El-Raheem[2]

[1]Department of Physics, Faculty of Sciences, Taif University, Taif, Saudi Arabia
[2]Physics Department, Faculty of Science, Sohag University, Sohag, Egypt
Email: *halkhammash@mail.com, khamash.h@tu.edu.sa

Abstract

Thin films of $Zn_{100-x}Cd_xO$ with x = 0, 2, 4, 6 and 8 at% were deposited by electron beam evaporation technique on glass substrates. The structural, optical and electrical properties of $Zn_{100-x}Cd_xO$ films with x = 4 at% have been investigated as a function of annealing temperature. Only zinc and cadmium appeared in the as-deposited films, by annealing their oxides found to exist. It was observed that the optical properties, such as transmittance, reflectance, optical band gap, and refractive index of $Zn_{100-x}Cd_x$, were strongly affected by annealing temperature. Other parameters named free carrier concentration, electrical resistivity of the films were studied as a function of annealing temperature for 4 at% CdO content. The figure indicates that the best value of annealing temperature is at 450°C.

Subject Areas

Experimental Physics

Keywords

$Zn_{100-x}Cd_xO$, Zinc

1. Introduction

Zinc and cadmium play an important role as alloying elements in many superconductor and semiconductor alloy properties [1] [2] as well as surface coating and plating process materials. These alloying elements are widely used for soldering processes, since many solders may contain Cd because of its low melting point, and also brazing processes, for higher temperatures, should use alloys containing large amounts of Zn. In particular, for lamellar eutectic alloys, Zn and Cd can exhibit some interesting properties. Furthermore, Zn-Cd eutectic

alloys have been widely used in many experimental studies [3]-[8], because of their low melting point and their regular lamellar structure.

Transparent conducting oxides (TCOs) are a class of materials that transmit visible radiation and conduct electricity. They find application as transparent electrodes in numerous applications such as photovoltaic, flat panel displays, heat reflective coatings on energy-efficient windows, and electrochromics such as smart mirrors [8] [9] [10] [11]. Zinc Oxide (ZnO) holds considerable interest as an optical transparent materials due to its wide band gap (3.3 ev), its amenability to defects or impurity doping and other desirable properties such as low cost and non-toxicity [12]. While pure ZnO films present high values of resistivity [13]. CdO is an n-type semiconductor, with a well-established direct band gap at approximately (2.4 - 2.7 ev) and a poor optical transmittance in the visible spectral region [3]. When compared with ZnO, the transmittance of CdO in the visible region of the spectrum has been reported as rather low. However, cadmium oxide is characterized by a much lower resistivity. Hence, it could directly combine the optical and electrical properties of an alloy of cadmium and zinc oxides, making it useful for its application in solar cells. This paper reports the preparation of Zn-doped Cd (where x = 0, 2, 4, 6 and 8 at%). The X-ray diffraction analysis, transmittance, optical band gap and electrical resistivity are measured to study the effect of the oxidation temperatures and the Ga-doping level. $Cd_xZn_{1-x}O$ films have been deposited by sol-gel spin-coating method onto glass substrates. It was observed that the crystal structure changed from wurtzite (ZnO) to cubic (CdO) structure [14]. $Zn_{0.8}Cd_{0.2}O$ thin films were deposited on glass substrates at different substrate temperatures (Ts) by the direct current (dc) reactive magnetron sputtering method. Results indicated that all the obtained thin films were of highly (002)-preferred orientation and possessing the hexagonal wurtzite structure of pure ZnO [15]. The ternary $Zn_{1-x}CdO$ (x: 0 - 1) alloy thin films were deposited on quartz substrate by the direct current reactive magnetron sputtering method. As x varied from x = 0.0 to 0.5, the $Zn_{1-x}Cd_xO$ thin films had a hexagonal wurtzite structure of pure ZnO and (002) preferred orientation. The optical band gap energies of the films were tuned from 3.24 eV at x = 0 to 2.04 eV at x = 0.5 [16]. The optical studies showed that the $Cd_xZn_{1-x}O$ thin films have optical transmittance in entire visible region. The resistivity of undoped films was very high and it decreased with addition of cadmium. The gas sensing properties were investigated at optimal temperature of 350°C for various volatile organic compounds like acetone, ethanol and methanol. The $Cd_xZn_{1-x}O$ thin films with 10 at% cadmium concentration showed the sensitivity of 50% for 1 ppm ethanol [17].

Electrical transport properties of CdO-ZnO thin film heterostructure have been studied. ZnO thin film deposited on conducting CdO thin film forms an n-n isotype heterostructure. The ZnO layer achieved significantly high electrical conductivity. A thin conducting channel is created in the interface at the ZnO side. Band bending near the interface creates electron accumulation at the ZnO

side giving rise to a highly conducting channel at the interface [18].

This work focuses on preparing $Zn_{100-x}Cd_xO$ thin films using e-beam evaporation method for CdO content at 0, 2, 4, 6 and 8 at%. The characterization, optical and electrical measurements will be carried out. The figure of merit will be studied as a function of annealing temperature.

2. Experimental Details

2.1. Preparation of the Thin Films

For preparing $Zn_{100-x}Cd_xO$ (x = 0, 2, 4, 6 and 8 at%) bulk samples, proper quantities of ZnO (99.98% purity) and CdO (99.95% purity) were sealed in an evacuated quartz ampoule and heated at 500˚C. Continuous stirring of the melt was carried out to ensure good homogeneity. The melt was then rapidly quenched in ice water. Thin films of the considered ratios were prepared by electron beam evaporation in an Edward's high vacuum coating unit model 306A under pressures of 5×10^{-6} and 8×10^{-5} Torr before and during film deposition, respectively. The films were deposited on an ultrasonically cleaned microscopic glasses held at room temperature. The thickness of the films (≈200 nm) was controlled using a digital film thickness monitor model TM 200 Maxtek. The deposition rate was ≈12.5 nm/s and then annealed in air for 1 h.

2.2. Characterization and Optical Measurements of the Thin Films

A Jasco model V-570 (UV-Visible-NIR) double beam Spectrophotometer (with photometric accuracy of ±0.002 - 0.004 Abs. and ±3% Trans.) was employed to record the transmission T and reflection R spectra over the wavelength range from 200 to 2500 nm at normal incidence. The absorption coefficient α of the films was determined directly from the spectrophotometer readings using the formula [19]:

$$\alpha = \frac{2.303}{d} \log 10 \left(\frac{1-R}{T} \right) \tag{1}$$

where d is the film thickness, T is the transmittance and R is the reflectance of the film.

The optical energy band gap E_g was estimated from the optical measurements by analyzing the optical data with the expression for the optical absorbance, and the photon energy, $h\upsilon$ using the following equation:

$$(\alpha h\upsilon)^2 = A(h\upsilon - E_g) \tag{2}$$

where α represents the absorption coefficient, h is the Planck s constant, and A is a constant, the values of E_g were obtained by extrapolating the linear portion of the plots of $(\alpha h\upsilon)^2$ versus $h\upsilon$ to $\alpha = 0$.

The refractive index n was calculated from the following equation:

$$n = \frac{1+R}{1-R} \pm \left[\left(\frac{R+1}{R-1} \right)^2 - (1+k^2) \right]^{1/2} \tag{3}$$

where $k = \alpha\lambda/4\pi$ is the extinction coefficient and λ is the incident light wavelength. In the present work, more reasonable values for n may be determined by considering the plus sign of Equation (3).

2.3. Measurements of the Electric Properties of the Thin Films

The resistivity measurements were carried out using a two-terminal configuration where the measurements were done at room temperature. Electrical contacts were made by applying silver paste over the surface of the films with a separation of 2 mm.

3. Results and Discussion

3.1. Characterization of the Thin Films

Figure 1 shows X-ray diffraction patterns of the as-prepared $Zn_{100-x}Cd_xO$ (x = 0, 2, 4, 6 and 8 at%) films. For the undoped ZnO film as seen in Figure 1(a) is polycrystalline with a hexagonal close-packed crystal lattice. The film has four prominent peaks of (002), (100), (101) and (004) plane with highly preferred orientation along the (002) direction as recorded in card No. 04-0831. As the concentration of CdO increases from x = 2 to 8 at% in the as-prepared $Zn_{100-x}Cd_xO$ thin films, the main peaks appear at 2θ = 31.635°, 66.34°, 36.15°, 38.74°, 43.029°, and 77.076°, which corresponded to Cd (002), (004) and Zn (002), (100), (101), (004) with highly preferred orientation along the (002) as seen in Figures 1(a)-(d). The intensity of the Cd (002) peak increases and becomes more and more prominent at x = 4 at% as shown in Figures 1(b)-(d).

The X-ray diffraction patterns of annealed $Zn_{100-x}Cd_x$ (x = 0, 2, 4, and 8 at%) thin films at 300°C for 1h are shown in Figures 2(a)-(d) indicate that, it possesses a polycrystalline hexagonal wurtzite structure with a preferred orientation along the ZnO_2 (200) plane at 2θ = 36.96. For x = 0.0, the peaks appear at 2θ = 33.88°, 35.02°, 36.96°, 39.71°, 43.94° and 77.62°, which correspond to Zn (002), (100), ZnO (200), Zn (100), ZnO_2 (101) and (004) planes respectively as seen in Figure 2(a). Doping Cd with x = 2%, three peaks appear at 2θ = 35.02°, 37.04° and 77.9° for Cd (100) and ZnO_2 (200), (004) respectively as shown in Figure 2(b). For x = 4% the main peaks appear at 2θ = 33.46°, 35.17°, 37.11° and 77.9° which corresponding to Cd (002), CdO_2 (200) and ZnO_2 (200), (004) plane respectively as clear in Figure 2(c). In additions, increasing x to 8 at%, the main peaks appear at 2θ = 32.44°, 36.98°, 39.06°, 43.91° and 77.78°, which corresponding to Cd (002), ZnO_2 (200), (004) and Zn (100) Zn (101) planes respectively as demonstrated in Figure 2(d). It is obvious that the crystal quality of the sample increases remarkably, and CdO (200) diffraction peak is observed, suggesting the phase segregation of CdO from the matrix phase [20]. Generally, this angular peak positions are greater than the as-prepare associated values. This trend can be ascribed to the tensile stresses that usually build in the furnace [21]. Also, the intensity ratio of ZnO and Cd peaks is decreased after annealing.

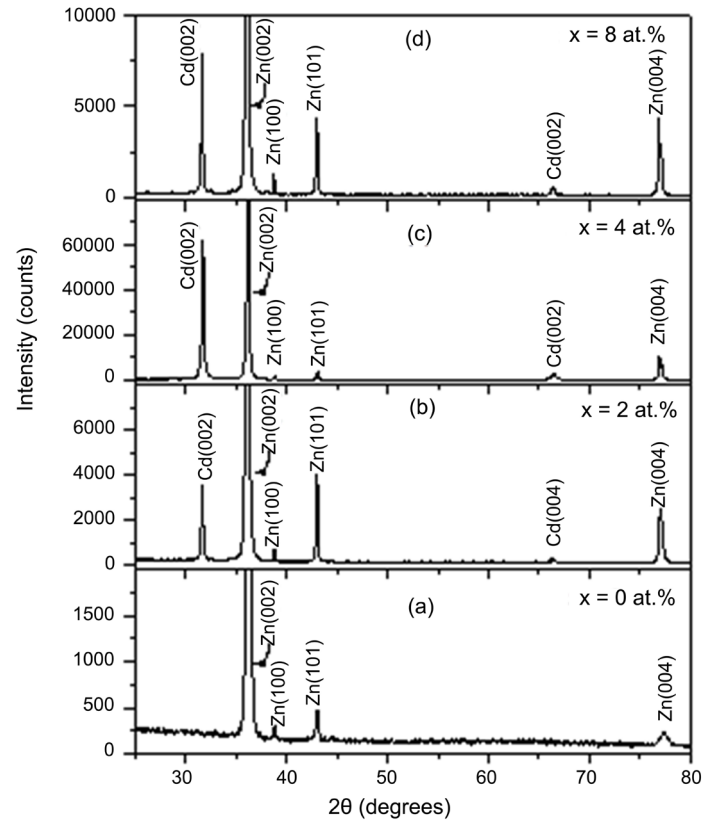The X-ray diffraction patterns of annealed $Zn_{100-x}Cd_x$ (x = 0, 2, 4, and 8 at%)

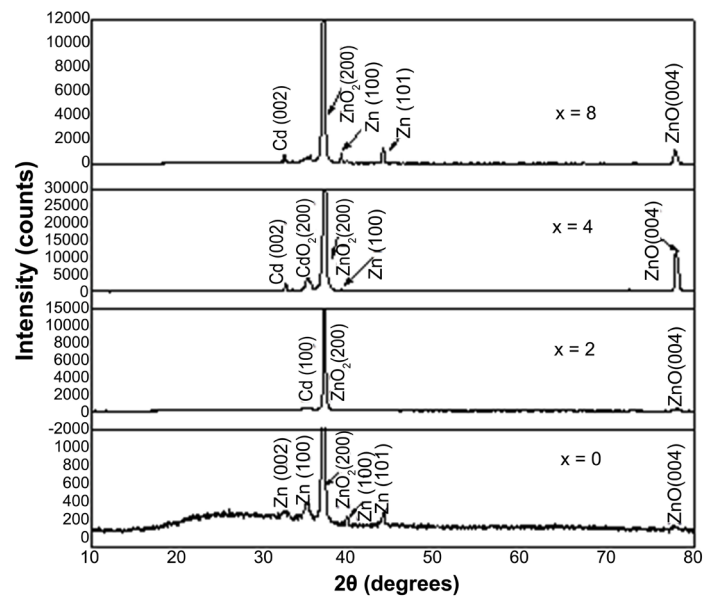**Figure 1.** X-ray diffraction of as deposited $Zn_{100-x}Cd_xO$ thin films.

Figure 2. X-ray diffraction of $Zn_{100-x}Cd_xO$ thin films annealing at 300˚C for 1 h.

films at 500˚C for 1h are shown in **Figures 3(a)-(d)** indicating that, it possesses a polycrystalline hexagonal wurtzite structure with a preferred orientation along the ZnO (002) direction. For **Figure 3(a)** undoped ZnO film the main peaks
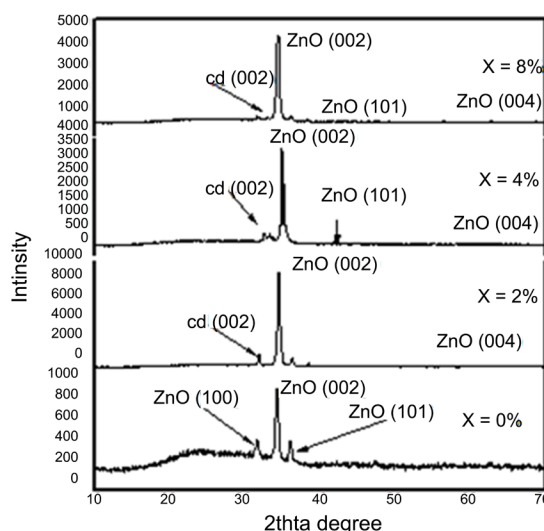
Figure 3. X-ray diffraction of $Zn_{100-x}Cd_x$ thin films annealing at 500˚C for 1 h.

appear at $2\theta = 31.50˚, 34.17˚, 35.95˚$ corresponding to ZnO in the direction (100), (002) and (101) plane. For x = 2% **Figure 3(b)** the main peaks appear at $2\theta = 31.75˚, 34.39˚$ for Cd (002) and ZnO (002) respectively.

Doping Cd with x = 4% as seen in **Figure 3(c)** the main peaks appear at $2\theta = 31.75˚, 34.39˚, 36.24˚, 38.32˚$ and $72.56˚$ which correspond to Cd (002), ZnO (200), ZnO (002), (101), (004) respectively. Finally, for x = 8% **Figure 3(d)** the main peaks appear at $2\theta = 31.54˚, 32.92˚, 34.31˚, 36.04˚$ and $72.46˚$ relating to Cd (002), ZnO (002), (002), (101) and (004) respectively.

From above, it is clear that Zn and Cd only appeared in the X-ray diffraction of the as-prepared films, whereas, ZnO and CdO are shown after annealing at 300˚C for 1 h, besides, ZnO and Cd exists in the X-ray diffraction patterns with annealing temperature 500˚ results in

3.2. Optical Properties of the Thin Films

The typical UV-VIS-NIR optical transmittance and reflectance spectra of an-nealed films ($Zn_{100-x}Cd_x$ with x = 4 at%) at different annealing temperature as a function of wavelength in the range from 300 to 2500 nm are shown in **Figure 4** and **Figure 5** respectively. It is clear that the transmittance increases and the reflectance decreases with increasing the annealing temperature from 200˚C to 450˚C. In **Figure 4**, the drop-off of the values of transmission belonging to the shorter wavelengths was related to the fundamental absorption by band-to-band transition. Meanwhile, the wavelength of the absorption edge decreased with an increase in temperature of annealing.

From the transmittance data it is possible to infer the optical energy gap of the films by plotting $(ahv)^2$ vs hv (where a is the absorption coefficient, and hv the photon energy) and by extrapolating the straight line portion of this plot to the energy axis. The obtained values have been plotted in **Figure 6**. The optical band gap E_g increases with increase in annealing temperature and found to be equal to
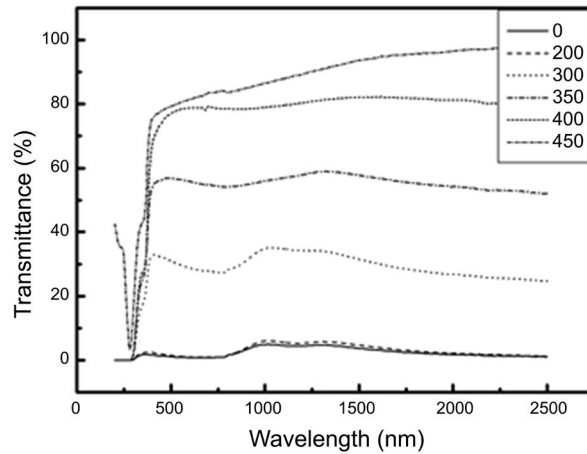
Figure 4. Spectral variation of the transmittance T% of annealed $Zn_{100-x}Cd_x$ (x = 4%) at different temperature.
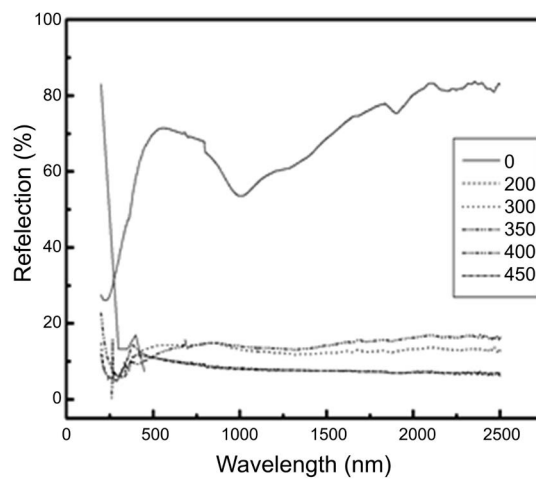

Figure 5. Spectral variation of the reflectance R% of annealed $Zn_{100-x}Cd_x$ (x = 4%) at different temperature.
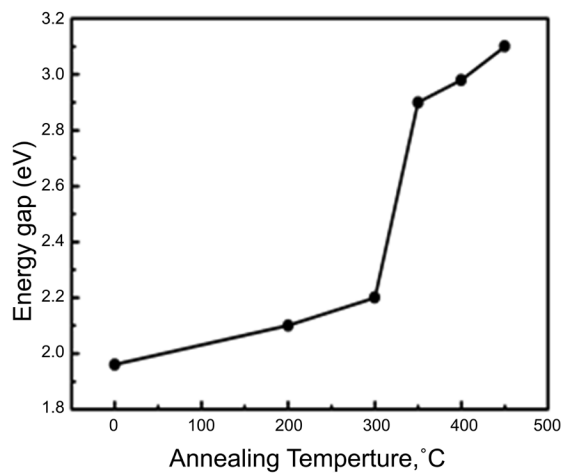

Figure 6. The variation of the Optical Band gap of the $Zn_{100-x}Cd_x$ (x = 4%) at different annealing temperature.

3.31 eV, which can be explained as follows: the unsaturated defects are gradually annealed out producing a larger number of saturated bonds leading to decreases in the density of localized states and consequently the optical gap increased [22].

The variations of refractive index and the extinction coefficient in the visible wavelength range of ($Zn_{100-x}Cd_x$ with x = 4 at%) films annealed at different temperature are depicted in Figure 7. The refractive index of the films decreases with increasing the annealing temperature which can be attributed to the decrease in the packing density with annealing temperature. On the other hand, the extinction coefficient (k) decreases with increasing the annealing temperature, which can be attributed to the increase of the film transparency [23].

The packing density *P* of the film can be estimated from the following equation [24]:

$$n_f^2 = \frac{(1-p)n_y^4 + (1+p)n_y n_s^2}{(1+p)n_y^2 + (1-p)n_s^2},$$

where n_f is the refractive index of $Zn_{100-x}Cd_x$ with x = 4 at% films, n_s is the refractive index of the solid part of the film, that for single crystal n_y Is the refractive index of the voids (equals one for air) and *P* is the packing density. It is observable also that the extinction coefficient decreases with increasing the annealing temperature. This could be correlated to the decrease of absorption with increasing the temperature of annealing, where $K = \lambda a/4\pi$ is the absorption coefficient [25].

3.3. Electrical of the Electrical Properties of the Thin Films

The dependence of electrical properties on the temperature of annealing is shown in Figure 8. The resistivity decreases as the temperature is increased up
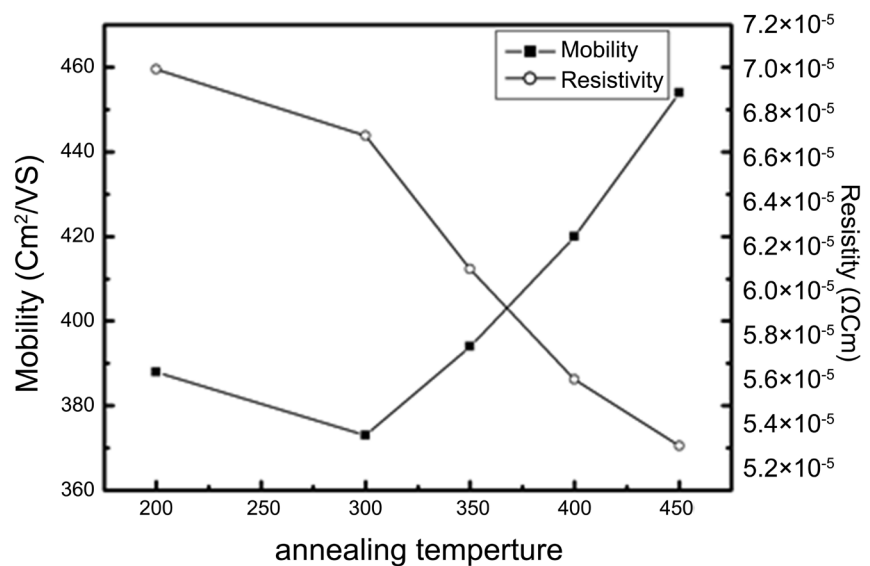

Figure 7. The variation of the mobility and resistivity of the $Zn_{100-x}Cd_x$ (x = 4%) at different annealing temperature.
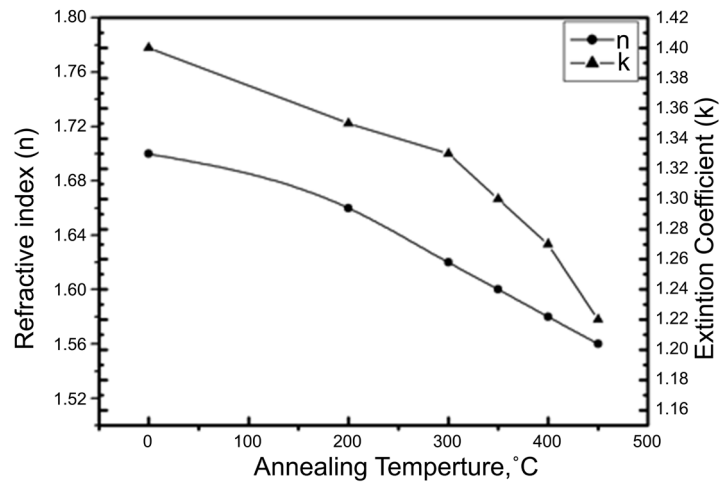
Figure 8. The variation of the of refractive index (n) and extinction coefficient (k) the $Zn_{100-x}Cd_x$ (x = 4%) at different annealing temperature.
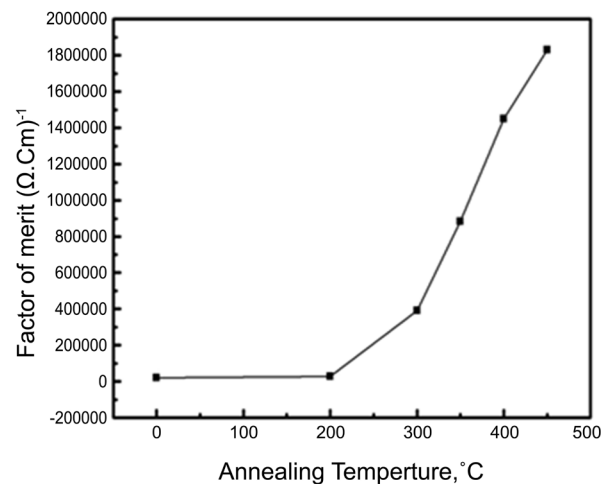

Figure 9. The variation of the Factor of merit of the $Zn_{100-x}Cd_x$ (x = 4%) at different annealing temperature.

to 450˚C showing semiconductor behavior. The lowest resistivity value $5.3 \times 10 - 5$ Ω-cm has been obtained for annealed film at temperature of 450˚C. It is observable also that, the carriers mobility increased with increase in annealing temperature. This may be due to the increase of the grain size with increase in annealing temperature, and this leads to reduction of the grain boundary scattering due to charge carriers. The decrease of the electrical resistivity of annealed films is due the increase of the mobility carriers.

In order to predict the selective properties of transparent conductive coatings from the fundamental optical and electrical properties, the factor of merit can be employed $\varphi = T_m / \rho$ [26] where T_m is the average transmittance in the visible region and ρ is the electrical resistivity. **Figure 9** shows the variation of the factor of merit as a function of annealing temperature. The figure indicates that the best value of annealing temperature is at 450˚C.

4. Conclusion

Thin films of $Zn_{100-x}Cd_xO$ with x = 0, 2, 4, 6 and 8 at% have been deposited by electron beam evaporation technique. The effect of heat treatment on the electrical, optical and structural properties of these films was carried out. For content of cadmium oxide at 4%, optical measurements indicated that, the optical energy gap, the mobility of the carriers, and the figure of merit increase with increasing the annealing temperature. On the other hand, our results indicate that, the refractive index, extinction coefficient, and the resistivity decrease with increasing the annealing temperature. The best value of the figure of merit found to be at annealing temperature 450˚C.

Conflicts of Interest

The authors declare no conflicts of interest regarding the publication of this paper.

References

[1] Sapoval, B. and Hermann, C. (1995) Physics of Semiconductors. Springer, New York. https://doi.org/10.1007/978-1-4612-4168-3

[2] Tiller, W.A. (1991) The Science of Crystallization. Vol. 1, Cambridge University Press, Cambridge.

[3] Shaw, B.J. (1967) Room Temperature Mechanical Properties of Cadmium-Zinc Lamellar Eutectic Alloys. *Acta Metallurgica*, **15**, 1169-1177. https://doi.org/10.1016/0001-6160(67)90391-4

[4] Sahoo, M., Porter, R.A. and Smith, R.W. (1976) Mechanical Behaviour of the Cd-Zn Eutectic Composite. *Journal of Materials Science*, **1**, 1680-1690. https://doi.org/10.1007/BF00737524

[5] Sahoo, M. and Smith, R.W. (1978) Mechanical Properties Characterization of the Pb-Cd Eutectic Composite. *Journal of Materials Science*, **13**, 283-290. https://doi.org/10.1007/BF00647771

[6] Cantor, B. and Chadwick, G.A. (1976) Thermal Stability of Eutectic and Off-Eutectic Ag-Cu, Cd-Zn and Al-ζ(AlAg) Alloys. *Journal of Crystal Growth*, **36**, 232-238. https://doi.org/10.1016/0022-0248(76)90282-7

[7] Van de Merwe, R.H., Smith, R.W., Lemkey, F.D., Cline, H.E. and Mc Lean, M. (Eds.) (1982) *In Situ* Composites IV. Elsevie Science Publishing, Co., Amsterdam, p. 291.

[8] Kaya, M. and Smith, R.W. (1989) The Discontinuous Coarsening Reactions in the Pb Cd and the Zn Cd Lamellar Eutectic Alloys-I. The Driving Force, Initiation and the Morphology. *Metall.*, **37**, 1657. https://doi.org/10.1016/0001-6160(89)90132-6

[9] Jayakrishnan, R. and Hodes, G. (2003) Non-Aqueous Electrodeposition of ZnO and CdO Films. *Thin Solid Films*, **440**, 19-25. https://doi.org/10.1016/S0040-6090(03)00811-3

[10] Biswasa, P.K., Dea, A., Pramanika, N.C., Chakraborty, P.K., Ortner, K., Hock, V. and Korder, S. (2003) Effects of Tin on IR Reflectivity, Thermal Emissivity, Hall Mobility and Plasma Wavelength of Sol-Gel Indium tin Oxide Films on Glass. *Materials Letters*, **57**, 2326-2332. https://doi.org/10.1016/S0167-577X(02)01220-X

[11] Yamammoto, S., Yamanaka, T. and Ueda, Z. (1987) Properties of Sn-Doped In_2O_3

by Reactive Magnetron Sputtering and Subsequent Annealing. *Journal of Vacuum Science & Technology A*, **5**, 1952. https://doi.org/10.1116/1.574889

[12] Sagar, P., Kumar, M. and Mehra, R.M. (2005) Influence of Hydrogen Incorporation in Sol-Gel Derived Aluminum Doped ZnO Thin Films. *Thin Solid Films*, **489**, 94-98. https://doi.org/10.1016/j.tsf.2005.05.009

[13] Vigil, O., Cruz, F., Santana, G., Vaillant, L., Morales-Acevedo, A., Choi, Y.S., Lee, C.G. and Cho, S.M. (1996) Transparent Conducting $Zn_xCd_{1-x}O$ Thin Films Prepared by the Sol-Gel Process. *Thin Solid Films*, **298**, 153. https://doi.org/10.1016/S0040-6090(96)08923-7

[14] Ilican, S., Caglar, Y., Caglar, M., Kundakci, M. and Ates, A. (2009) Photovoltaic Solar Cell Properties of $Cd_xZn_{1-x}O$ Films Prepared by Sol-Gel Method. *International Journal of Hydrogen Energy*, **34**, 5201-5207. https://doi.org/10.1016/j.ijhydene.2008.10.022

[15] Sui, Y.R., Yue, Y.G., Cao, Y., Yao, B., Liu, X.Y., Lang, J.H., Gao, M., Li, X.F., Li, X.Y. and Yang, J.H. (2014) Influence of Substrate Temperature on Structural and Optical Properties of ZnCdO Thin Films Deposited by DC Magnetron Sputtering. *Ceramics International*, **40**, 9189. https://doi.org/10.1016/j.ceramint.2014.01.136

[16] Sui, Y., Yue, Y., Song, Y., Cao, Y., Yao, B., Lang, J., Li, X. and Yang, J. (2015) Effects of Cd Concentration on Microstructure and Optical Properties of the Ternary Zn1-xCdxO Alloy Thin Films Synthesized by Magnetron Sputtering. *Materials Research Bulletin*, **70**, 348-353. https://doi.org/10.1016/j.materresbull.2015.05.004

[17] Bharath, S.P., Bangera, K.V. and Shivakumar, G.K. (2017) Properties of $Cd_xZn_{1-x}O$ Thin Films and Their Enhanced Gas Sensing Performance. *Journal of Alloys and Compounds*, **720**, 39. https://doi.org/10.1016/j.jallcom.2017.05.240

[18] Bera, A., Thapa, R., Chattopadhyay, K.K. and Saha, B. (2015) In Plane Conducting Channel at the Interface of CdO-ZnO Isotype Thin Film Heterostructure. *Journal of Alloys and Compounds*, **632**, 343-347. https://doi.org/10.1016/j.jallcom.2015.01.168

[19] Ali, H.M. (2005) Characterization of a New Transparent-Conducting Material of ZnO Doped ITO Thin Films. *Physica Status Solidi A*, **202**, 2742-2752. https://doi.org/10.1002/pssa.200521045

[20] Ma, D.W., Ye, Z.Z., Huang, J.Y., Zhu, L.P., Zhao, B.H. and He, J.H. (2004) Effect of Post-Annealing Treatments on the Properties of $Zn_{1-x}Cd_xO$ Films on Glass Substrates. *Materials Science and Engineering B*, **111**, 9-13. https://doi.org/10.1016/j.mseb.2003.12.007

[21] Gupta, V. and Mansingh, J. (1996) Influence of Postdeposition Annealing on the Structural and Optical Properties of Sputtered Zinc Oxide Film. *Applied Physics*, **80**, 1063. https://doi.org/10.1063/1.362842

[22] Ali, H.M., Abd-Raheem, M.M., Megahed, N.M. and Mohamed, H.A. (2006) Optimization of the Optical and Electrical Properties of Electron Beam Evaporated Aluminum-Doped Zinc Oxide Films for Opto-Electronic Applications. *Journal of Physics and Chemistry of Solids*, **67**, 1823-1829. https://doi.org/10.1016/j.jpcs.2006.04.005

[23] Mohamed, H.A., Ali, H.M., Mohamed, S.H. and Abd El-Raheem, M.M. (2006) Transparent Conducting ZnO-CdO Thin Films Deposited by e-Beam Evaporation Technique. *The European Physical Journal Applied Physics*, **34**, 7-12. https://doi.org/10.1051/epjap:2006039

[24] Maclend, H.A. (1986) Structure-Related Optical Properties of Thin Films. *Journal of Vacuum Science & Technology A*, **4**, 418. https://doi.org/10.1116/1.573894

[25] Abu El-Fadl, A., Mohamad, G.A., Abd El-Moiz, A.B. and Rashad, M. (2005) Optical

Constants of $Zn_{1-x}Li_xO$ Films Prepared by Chemical Bath Deposition Technique. *Physica B*, **366**, 44. https://doi.org/10.1016/j.physb.2005.05.019

[26] Ali, H.M., Mohamed, H.A. and Mohamed, S.H. (2005) Enhancement of the Optical and Electrical Properties of ITO Thin Films Deposited by Electron Beam Evaporation Technique. *The European Physical Journal Applied Physics*, **31**, 87. https://doi.org/10.1051/epjap:2005044